frontiers | Frontiers in Energy Research

ORIGINAL RESEARCH
published: 26 April 2022
doi: 10.3389/fenrg.2022.837160

Synthesis of Micron-Sized NiAl/NiCoAl-Layered Double Hydroxides *via* a Facile Double Hydrolysis Dropping Method for Supercapacitor Applications

Xiaowei Huang[1], *Wenfeng Xiang*[1]*, *Jiangfeng Yao*[1] *and Jianfeng Xi*[2]

[1]Beijing Key Laboratory of Optical Detection Technology for Oil and Gas, China University of Petroleum, Beijing, China, [2]Department of Physics, Beijing Technology and Business University, Beijing, China

The transition metal-based layered double hydroxides (LDHs) for high-performance supercapacitor applications were synthesized by the double hydrolysis dropping method. We found that the dropping sequence of the cation and anion solutions has a strong influence on the microstructural and electrochemical properties of LDHs. The NiAl LDHs obtained by dropping the Ni^{2+} solution into the AlO^{2-} solution have obvious layered structures with a particle size of the order of micrometers. They are different from those LDHs prepared by the conventional double hydrolysis method and hydrothermal method. The specific capacity of the NiAl LDHs is about 615 C g^{-1} at 0.5 A g^{-1}, which is almost twice that of the sample synthesized by the traditional double hydrolysis method (339 C g^{-1}). It is indicated that the performance of the NiAl LDHs is improved by the dropping method. Moreover, an excellent cyclic stability of 83.3% capacitance retention after 1000 cycles at 3 A g^{-1} was achieved. In addition, the trimetallic NiCoAl LDHs have been synthesized successfully by the dropping method. The results showed that the addition of Co effectively enhanced the electrochemical properties of LDHs. The optimal NiCoAl LDHs display an excellent specific capacity of 990 C g^{-1} at 0.5 A g^{-1}. This work offers an efficient and facile route, without hydrothermal treatment or adscititious alkali sources, to fabricating LDHs for boosting energy storage capabilities.

Keywords: NiAl/NiCoAl layered double hydroxides, supercapacitors, dropping method, microstructures, electrochemical properties

OPEN ACCESS

Edited by:
Manickam Minakshi,
Murdoch University, Australia

Reviewed by:
Ashok M,
National Institute of Technology, India
Hai Wang,
Murdoch University, Australia

***Correspondence:**
Wenfeng Xiang
wfxiang@cup.edu.cn

Specialty section:
This article was submitted to Electrochemical Energy Conversion and Storage, a section of the journal Frontiers in Energy Research

Received: *16 December 2021*
Accepted: *21 March 2022*
Published: *26 April 2022*

Citation:
Huang X, Xiang W, Yao J and Xi J (2022) Synthesis of Micron-Sized NiAl/NiCoAl-Layered Double Hydroxides via a Facile Double Hydrolysis Dropping Method for Supercapacitor Applications. Front. Energy Res. 10:837160. doi: 10.3389/fenrg.2022.837160

INTRODUCTION

For the past few decades, electrochemical supercapacitors have attracted worldwide research interest due to the wide applications in small and medium electronics (Theiss et al., 2016; Yang et al., 2017; Huang et al., 2018). Electrode materials are considered to be the key factors affecting the performance of supercapacitors (Zhang et al., 2017). The morphology, size, porosity, and conductivity of electrode materials have a great influence on the rate capability, discharge/charge rates, and cycling stability of supercapacitors (Patil et al., 2017). Many kinds of materials, including carbon materials (Lee et al., 2013; Bashid, et al., 2017), conducting polymers (Dubal et al., 2012; Tan et al., 2018), and transitional metal oxides (Kim et al., 2012; Gopalakrishnan et al., 2017), have been developed for the application

of electrodes. However, the preparation of these materials requires expensive raw materials and/or complicated manufacturing techniques.

Recently, layered double hydroxides (LDHs) have attracted much more attention in design of electrodes (Li et al., 2016; Tyagi et al., 2019). The structural formula of LDHs is $[M_{1-x}^{2+} M_x^{3+} (OH)_2] (A_{x/n}^{n-} \cdot mH_2O)$, of which M^{2+} is the divalent metallic cation (such as Co^{2+}, Zn^{2+}, Ni^{2+}, etc.), M^{3+} is the trivalent metallic cation (such as Al^{3+}, Mg^{3+}, Fe^{3+}, etc.), and A^{n-} is the anion (such as Cl^-, OH^-, SO_4^{2-}, CO_3^{2-}, etc.) arranged in the interlayer (Wang X. et al., 2017; Shang et al., 2019). Among these LDHs, Ni- and/or Co-based LDHs exhibit excellent electrochemical performance due to their high specific capacity, good cycling stability, and rate capability (Li et al., 2018). Meanwhile, the trimetallic LDHs composed of two kinds of transition metals exhibit higher electrochemical and electrocatalytic performances compared with the bimetallic counterparts (Gonçalves et al., 2020). Ding et al. reported that doping Co species could effectively enhance the electronic and ionic conductivity and deprotonation of NiAl-LDHs (Ding t al., 2018). Gupta et al. also found that the specific capacity of NiCoAl LDHs was higher than those of NiAl LDHs and CoAl LDHs (Gupta et al., 2009).

LDHs can be synthesized by many methods, such as co-precipitation, urea hydrolysis, sol-gel methods, hydrothermal methods, and chemical stripping methods (Wang et al., 2015; Wang et al., 2017b; Hou et al., 2018; Sokol et al., 2019). However, most of the methods require high-temperature, high-pressure environments and adscititious alkali sources. As a low-cost, environmentally friendly, safe, and feasible method, the double hydrolysis method was used to synthesize composite hydroxides without any adscititious alkali sources and heat-treatment processes (Gu et al., 2015; Yang et al., 2016). However, the hydroxides with layered structures have not been reported by using the double hydrolysis method.

Nowadays, in order to control the size, microstructure, and morphology of materials, great efforts have been made in synthesizing nanomaterials by the dropping method (Bashiri-Shahroodi et al., 2008; Sharonova et al., 2016; Li et al., 2019). By controlling the Ni^{2+} concentration and the precursor solution addition, the diameter of Ni nanowires has been tuned from 85 to 350 nm (Xiang et al., 2017). Kumar et al. reported that the morphology and particle size of high energetic compounds can be effectively controlled by using drop-by-drop and drop-to-drop solvent–antisolvent interaction methods (Raj et al., 2019).

In this paper, combined with the advantages of the double hydrolysis method and dropping method, the micron-sized NiAl/NiCoAl LDHs were synthesized by a dropping double hydrolysis process. The effect of the dropping sequence of solutions on the microstructural and electrochemical properties of LDHs has been investigated. The optimal NiAl LDHs have a remarkable specific capacity of 615 C g^{-1} at 0.5 A g^{-1}. Moreover, they retain 83.3% of the original specific capacity even after 1000 cycles. In addition, the specific capacity of the NiCoAl LDHs was up to 990 C g^{-1} at 0.5 A g^{-1}.

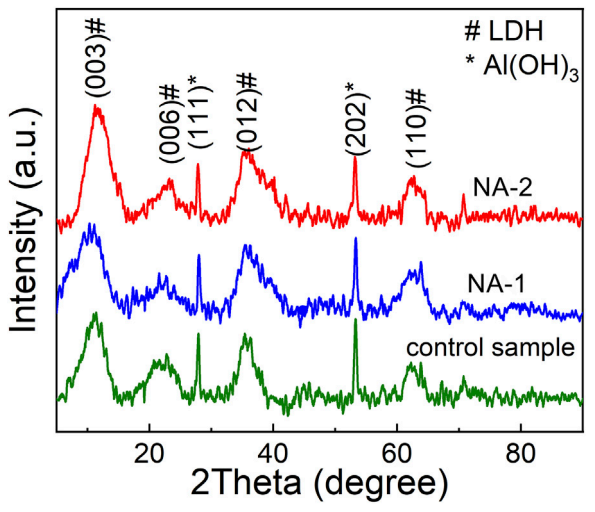

FIGURE 1 | XRD patterns of the control, NA-1, and NA-2 samples.

EXPERIMENTAL

Materials Synthesis

Nickel chloride ($NiCl_2.6H_2O$), sodium metaaluminate ($NaAlO_2$), cobalt chloride ($CoCl_2.6H_2O$), graphite, and polytetrafluoroethylene (PTFE, 60 wt%) were purchased from Shanghai Chemical Co., Ltd., China. All chemicals were of analytical grade and used as received without any purification. The NiAl and NiCoAl LDHs were synthesized by the dropping double hydrolysis method. First, 0.02 mol $NaAlO_2$ and 0.01 mol $NiCl_2.6H_2O$ were dissolved in 400 and 100 ml distilled water under continuous magnetic stirring to form solution A and solution B, respectively. Then, the NiAl LDHs were prepared by using the dropping method with two different adding sequences of reactants. When solution A was added dropwise into solution B, the products were denoted as NA-1. Conversely, the products were denoted as NA-2 when solution B was added dropwise into solution A. In addition, the control sample was synthesized by the traditional method. For the trimetallic NiCoAl LDH synthesis, solution B was prepared with the mixture of $NiCl_2.6H_2O$ and $CoCl_2.6H_2O$ with the volume ratio of 1:1, and the products were denoted as NCA-3. At the same time, the CoAl LDHs were synthesized, denoted as CA-4. It should be noted that solution B was added dropwise into solution A in their synthesis processes. Finally, all the mixed solutions were continuously stirred for 24 h at room temperature. After filtration and vacuum drying at 40°C for 10 h, the powder products were collected.

Physical and Electrochemical Characterization Techniques

X-ray powder diffraction (XRD) measurements were conducted by using a Bruker D8 diffractometer. Scanning electron microscopy (SEM, ZEISS, SIGMA 500, GER) and the corresponding energy-dispersive X-ray spectrometry (EDS, Bruker, GER) were used to characterize the microstructure

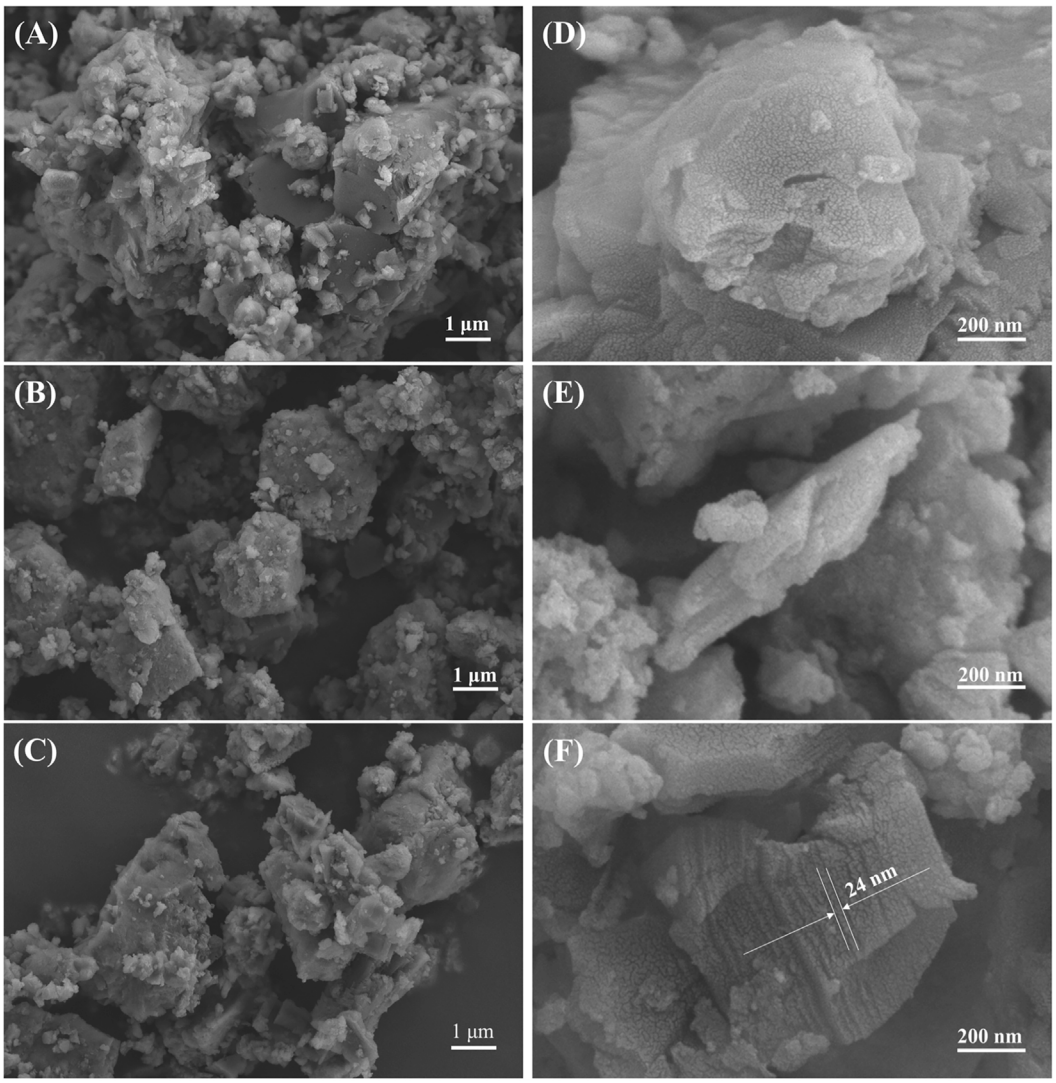

FIGURE 2 | SEM images of the **(A,D)** control, **(B,E)** NA-1, and **(C,F)** NA-2 samples.

and element distribution of the products at 10 kV. All electrochemical measurements were performed using an electrochemistry workstation (CHI660E, Chenhua, Shanghai, China). The electrochemical measurements were made in 6 M NaOH electrolyte at room temperature. A standard three-electrode system was used, which included the NiAl/NiCoAl LDH-coated Ni foam as the working electrode, a saturated Hg/HgO electrode as the reference electrode, and a platinum plate as the counter electrode. To prepare the working electrode, NiAl/NiCoAl LDHs, graphite, and PTFE were mixed with a weight ratio of 7:2:1 in absolute ethyl alcohol, and then the mixture was smeared onto a 1 cm × 1 cm Ni-foam substrate. After drying at 40°C for 2 h, the electrode was pressed with a pressure of 2 MPa. The mass loading of NiAl LDHs/NiCoAl LDHs on the Ni-foam substrate was 5 mg/cm^2. Cyclic voltammetry (CV) curves were measured within a potential region of 0–0.6 V with the scanning rates of 5, 10, 20, 50, and 100 mV s^{-1}. The galvanostatic charge–discharge (GCD) curves were measured from 0 to 0.5 V with different current densities. The cycle-life test was performed by the GCD measurement between 0 and 0.5 V with a current density of 3 A g^{-1} for 1000 cycles. Electrochemical impedance spectroscopy (EIS) was conducted under an AC voltage of 5 mV with the frequency range from 10^{-2} to 10^5 Hz. The specific capacity (SC) of the active material was calculated through the CV curves using the following equation (Brousse, et al., 2015; Zhang et al., 2019):

$$SC_1 = \frac{\int idV}{mv} \tag{1}$$

where i is the current density (A g^{-1}), V is the voltage (V), v is the scanning rate (mV/s), and m (g) is the mass of the electrode material. In addition, GCD curves were also used to calculate the SC by the equation

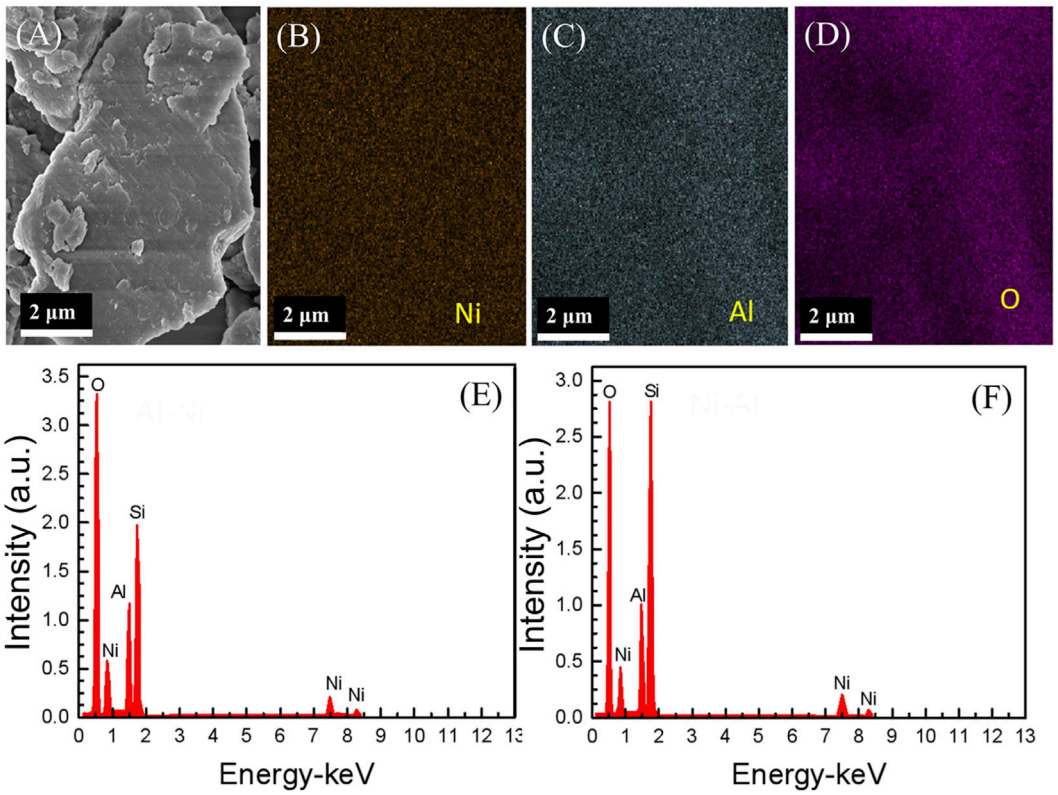

FIGURE 3 | (A) SEM imaging and **(B–D)** EDS mapping of the NA-2 sample and EDS patterns of the **(E)** NA-1 and **(F)** NA-2 samples.

$$SC_2 = \frac{I\Delta t}{m} \tag{2}$$

where I is the discharge current, Δt (s) is the discharge time, and m (g) is the mass of the electrode material.

RESULTS AND DISCUSSION

The Structural and Electrochemical Properties of the NiAl LDHs

Figure 1 shows the XRD patterns of the NiAl LDHs. The diffraction peaks at 2θ = 11.6°, 23.4°, 34.4°, and 60.5° can be assigned to the (003), (006), (012), and (110) reflections of LDHs, respectively, which are consistent with the standard card JCPDS-40-0216. The coexistence of the (003) and (006) diffraction peaks indicates that the NiAl LDHs are a layered structure (He et al., 2015; Pan et al., 2018). Specially, the diffraction peak intensity of the NA-2 sample is higher than that of the NA-1 and control samples, indicating that the NA-2 sample has better crystallinity. In addition, the $Al(OH)_3$ diffraction peaks occurred in the patterns, suggesting that there is a small amount of $Al(OH)_3$ impurities in samples besides the LDH phase.

Figures 2A–C show the SEM images of the samples. The particle sizes of all samples are similar, and the largest particle size is ~4 μm. As discerned from the magnification SEM images shown in **Figures 2D,E**, no clearly layered structures were found for the control and NA-1 samples; however, the NA-2 sample has a distinctive layered structure with a layer thickness of 24 nm (**Figure 2F**), which is in agreement with the results of XRD. It can be found that from **Figures 3B–D**, the atomic species in the NA-2 sample are uniformly distributed. **Figures 3E,F** show that only the Ni, Al, and O elements were observed. Moreover, the molar ratio of Ni to Al for the NA-1 and NA-2 samples is 1:2.68 and 1:2.16, respectively.

The typical CV curves with different scanning rates are shown in **Figures 4A–C**. A set of intense redox peaks were found for all samples, implying that the NiAl LDH electrodes have typical battery-type electrochemical characteristics. At the scanning rate of 5 mV s^{-1}, the anodic oxidation peaks and cathodic reduction peaks located at 0.2–0.3 V and 0.4–0.5 V are observed, respectively. Moreover, the anodic peaks shift further toward the negative side as the scanning rate increases. On the contrary, the cathodic peaks shift toward the positive side. It is indicated that a reversible Faradic process occurred. As shown in **Figure 4D**, the SC values of the control, NA-1, and NA-2 samples calculated from CV curves are 831, 993, and 1124 C g^{-1} at a scanning rate of 5 mV s^{-1}, respectively. With the increase of scanning rate, the value of SC decreased. When the scanning rate rose to 100 mV s^{-1}, the SC values of the three samples went down to 162, 173, and 149 C g^{-1}, respectively. In addition, the retention rate of the three samples is 20, 17, and 13%, respectively.

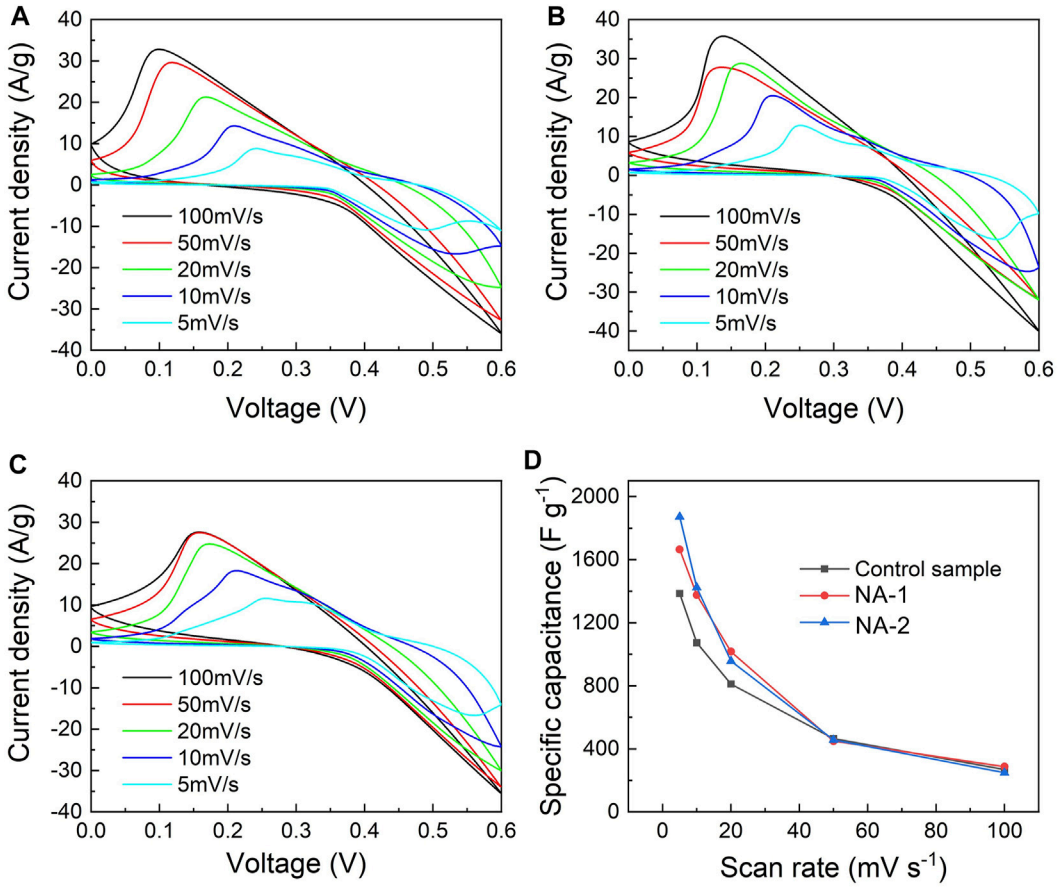

FIGURE 4 | CV curves at the scanning rate of 5–100 mV s^{-1} of the **(A)** control, **(B)** NA-1, and **(C)** NA-2 samples and **(D)** scanning rate dependence of specific capacity for the control, NA-1, and NA-2 samples.

Figures 5A–C show the GCD curves of the samples. The charge/discharge curves were nonlinear, which further confirms that the redox reaction occurs during the process. Moreover, a voltage platform at 0.3–0.4 V in figures is observed. The discharge time of the control, NA-1, and NA-2 samples at 0.5 A g^{-1} is 1700, 1900, and 2400 s, respectively. It can be found that the NA-2 sample possesses the longest discharge time, that is, the NA-2 sample has a good charge-storage performance compared to the other two samples. **Figure 5D** presents the calculated SC values of the three samples at various discharge current densities. The values of SC are 339, 483, and 615 C g^{-1} at a current density of 0.5 A g^{-1}, respectively. Compared to the control sample, the SC of the NA-1 and NA-2 samples is increased by 43 and 81%, respectively. With the increase of the current density, the SC of all samples decreased. When the current density increased to 5 A g^{-1}, the values of SC decreased to 230, 341, and 403 C g^{-1}, respectively. The retentions of the three samples reached up to 67.8%, 70.4% and 65.7% as the current density increased from 0.5 to 5 A g^{-1}, respectively. Based on the results of CV and GCD curves, we found that the SC values of the samples synthesized by the dropping method were higher than that of the control sample. Moreover, the NA-2 sample exhibits a higher SC among the three samples.

Figure 6 presents the SC retention of the three samples with 1000 cycles at a current density of 3 A g^{-1}. The SC retention change of the NA-1 and NA-2 samples is evidently different from that of the control sample. With the increase of cycling number, the SC values of the NA-1 and NA-2 samples increase initially and then gradually decrease, indicating that the two samples have an activation process. During the activation process, the number of the available active sites is increased. With the increase of cycling number, many available active sites were gradually trapped (Zheng et al., 2016). For the control sample, the SC decreases with the increasing cycling numbers, but the decrement is diminishing. In addition, the SC retention of the NA-2 sample is 83.3% after 1000 cycles, which is better than that of the control (66.7%) and NA-1 (74.4%) samples. In addition, **Supplementary Table S1** in the Supporting Information shows the comparison of the electrochemical properties of NiAl and NiCoAl LDHs synthesized by different methods. It can be seen that the NA-2 sample has a higher SC and a brilliant SC retention.

Based on these above results, it can be found that the supercapacitive performance of the samples synthesized by the dropping method is evidently greater than that of the control sample. It mainly results from their different microstructures. As shown in **Figure 2**, the NA-2 sample has a clearly layered

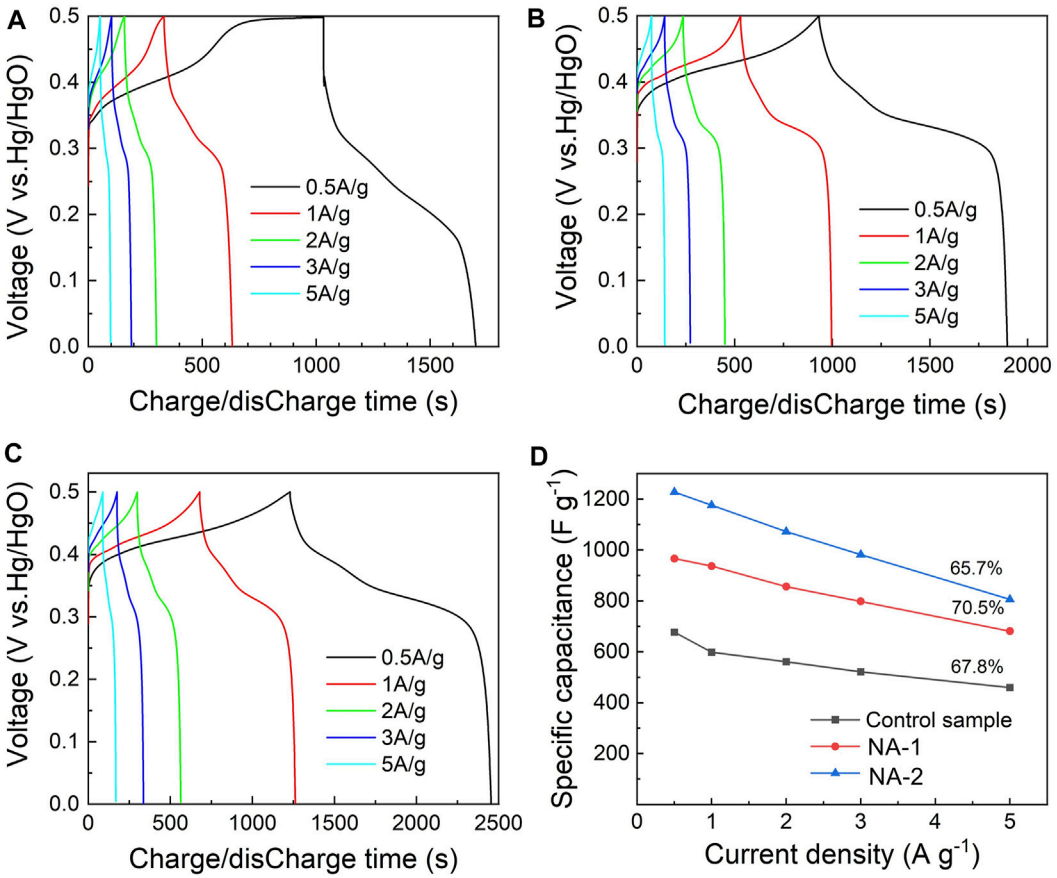

FIGURE 5 | GCD curves of the **(A)** control, **(B)** NA-1, and **(C)** NA-2 samples and **(D)** specific capacity of the control, NA-1, and NA-2 samples versus the current densities.

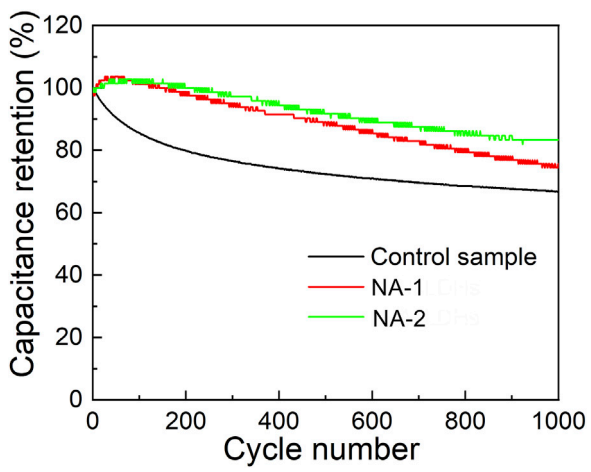

FIGURE 6 | Long-term cycling stability determined a current density of 3 A g^{-1} for the control, NA-1, and NA-2 samples.

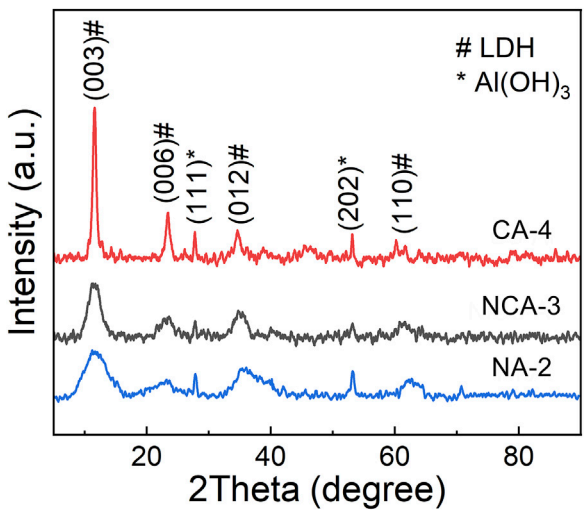

FIGURE 7 | XRD patterns of the NA-2, NCA-3, and CA-4 samples.

structure compared to the control sample. In the layered structure, the ions can be quickly transported by the interlayer spacing. Therefore, the ion-exchange capability and large-current discharging performance of the samples are improved (Gao et al., 2019). In addition, the performance of the NA-2 sample is better than that of the NA-1 sample. This is to say, the dropping

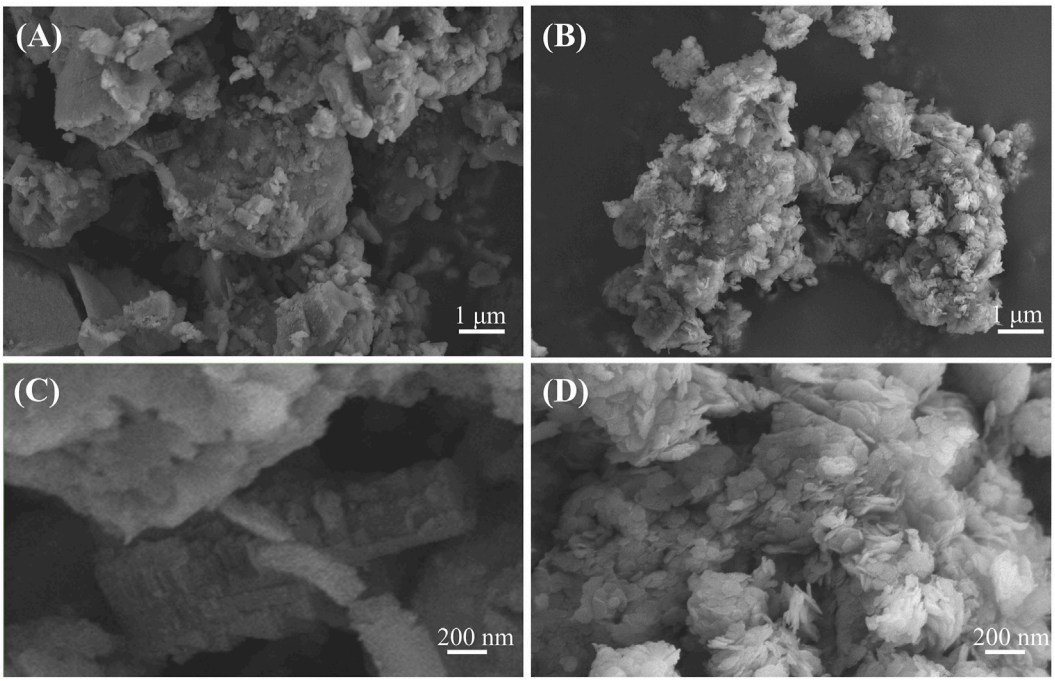

FIGURE 8 | SEM images of the **(A,C)** NCA-3 and **(B,D)** CA-4 samples.

sequence of the solvent has an effective influence on the properties of the samples, which possibly results from the difference of Al content in both samples. The EDS measurements showed that the content of Al of the NA-1 sample is slightly larger than that of the NA-2 sample. Since Al is not electroactive, it has not a direct impact on Faradic redox reaction (Gao et al., 2019). The increase of Al content may decrease the number of surface active sites and hinder the redox reaction (Wang et al., 2017a).

The Structural and Electrochemical Properties of NiCoAl LDHs

Figure 7 shows XRD patterns of the NCA-3 and CA-4 samples. The diffraction patterns of the samples are similar to that of the NA-2 sample. The increase of diffraction peak intensity with the addition of Co content indicated that the crystallinity of the samples was improved. Surface morphologies of the samples are investigated in **Figure 8**. Similarly, the microstructures of the NCA-3 sample are the micron-size particles with a layered structure. It is interesting to note that the structure of the CA-4 sample is evidently different from that of the NA-2 and NCA-3 samples. It is a nanosheet structure with a diameter of ~100 nm (**Figures 8B,D**), which is similar to that synthesized by the hydrothermal method (Su et al., 2019). The results indicated that the synthesis mechanism of the CA-4 sample is completely different from that of the NA-2 and NCA-3 samples.

The CV curves of the NCA-3 and CA-4 samples with different scanning rates are shown in **Figures 9A,B**, respectively. There are two anodic oxidation peaks and two cathodic reduction peaks for the NCA-3 sample observed at a scanning rate of 5 mV s^{-1}. It indicated that both $Ni(OH)_2$ and $Co(OH)_2$ were involved in the Faradaic reactions. However, only one anodic oxidation peak and one cathodic reduction peak occurred for the CA-4 sample. The SC of the NCA-3 sample at a scanning rate of 5 mV s^{-1} is 1743 C g^{-1}, which is higher than that of the CA-4 sample (1354 C g^{-1}).

Figures 9C,D show the GCD curves with different discharge current densities. At the current density of 0.5 A g^{-1}, the SC values of the NCA-3 and CA-4 samples were determined to be 990 and 854 C g^{-1}, respectively. It can be seen that the SC of the NCA-3 sample is higher than that of the NA-2 and CA-4 samples, which might be attributed to the addition of Co. Compared to the NiAl LDHs, the interlayer spacing of the NiCoAl LDHs was enlarged, which induced a fast diffusion rate of OH^- ions during the charging/discharging process (Ding et al., 2018). In addition, it is pointed out that the SC of the NCA-3 sample is obviously larger than that of other NiCoAl LDHs reported in the literature concerned, as shown in **Supplementary Table S1** in the Supporting Information. It possibly results from the distinctive layered structures of the NCA-3 sample. When the current density rises to 5 A g^{-1}, the specific capacity and the capacitance retention of the NCA-3 sample are 122 C g^{-1} and 12.3%, respectively. The retention rate of the NCA-3 sample is slightly lower than those reported by other groups (Xu et al., 2014; Bai et al., 2017; Tian et al., 2020), which possibly results from the low conductivity of the electrodes. In our experiments, the electrodes were fabricated by the pure NiCoAl LDHs. It has a low conductivity compared to the electrodes mixed by the NiCoAl LDHs and reduced graphene oxide, 3D graphene, and

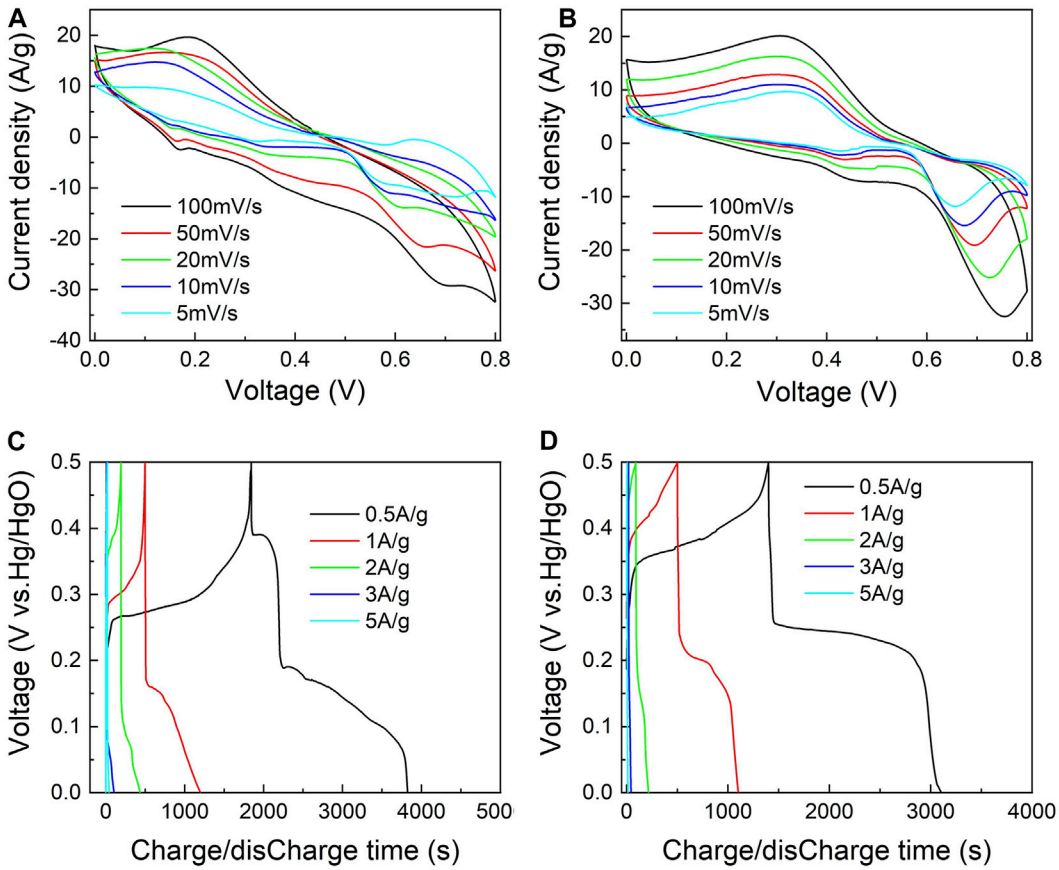

FIGURE 9 | CV curves of the **(A)** NCA-3 and **(B)** CA-4 samples with different scanning rates and GCD curves of the **(C)** NCA-3 and **(D)** CA-4 samples.

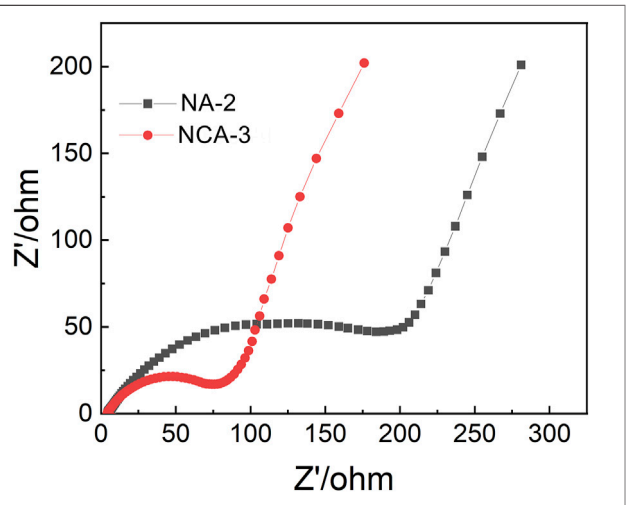

FIGURE 10 | Nyquist plots of the EIS data for the NA-2 and NCA-3 samples.

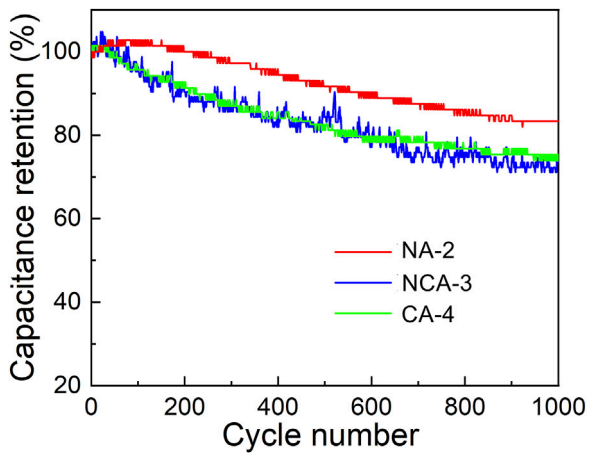

FIGURE 11 | Long-term cycling stability under a current density of 3 A g^{-1} for the NA-2, NCA-3, and CA-4 samples.

graphene nanosheets (Guo et al., 2019). Therefore, a greater diffusion resistance in the intercalation or deintercalation processes leads to a lower SC retention rate.

EIS was adopted to investigate the kinetic properties of electrodes. As shown in **Figure 10**, two distinct parts including a semicircle in the high-frequency region (charge-transfer process) and a sloped straight line in the low-frequency region (diffusion-limited process)

were found. In terms of the intercept with the real axis of plots, two electrodes possess a relatively low equivalent series resistance. In comparison with the NA-2 sample, the NCA-3 sample has a smaller semicircle diameter. It suggested that the addition of Co decreases the charge-transfer resistances. **Figure 11** displays the test results of 1000 charge/discharge cycles for the NCA-3, CA-4, and NA-2 samples at the current density of 3 A g^{-1}. The capacity retentions of these samples were 73.5, 75.4 and 83.3%, respectively. It can be seen that the capacity retentions of the NCA-3 and CA-4 samples are slightly smaller than that of the NA-2 sample.

CONCLUSION

We have successfully synthesized the micron-sized NiAl and NiCoAl LDHs for supercapacitors by the double hydrolysis dropping method. The microstructures of NiAl and NiCoAl LDHs are obviously different from that synthesized by the conventional double hydrolysis methods. Moreover, the electrochemical performances of LDHs were improved. The NA-2 sample has a superb capacity performance of 615 C g^{-1} at 0.5 A g^{-1} and excellent cycling performance (a capacity retention of 83.3%) due to its the uniform and ultra-thin layered structures with a layer thickness of 24 nm. The microstructural and electrochemical properties of LDHs have been influenced by the dropping sequence of the cation and anion solutions. The electrochemical performance of the NA-2 sample is distinctively different from that of the NA-1 sample. The SC of the NCA-3 sample was improved by the addition of Co. However, the capacity retention decreased. In addition, the nanosheet structure of the CA-4 sample is different from the micron-sized layer structure of the NA-2 and NCA-3 samples, which indicated that the synthesis mechanism is different. This improved synthesis method shows a great potential value to synthesized LDHs with excellent supercapacitive performance.

DATA AVAILABILITY STATEMENT

The original contributions presented in the study are included in the article/**Supplementary Material,** further inquiries can be directed to the corresponding author.

AUTHOR CONTRIBUTIONS

XH and WX contributed to conception and design of the study. JY specifically performed the experiments. JX performed the statistical analysis. XH wrote the first draft of the manuscript. XH, WX, JY, and JX wrote sections of the manuscript. All authors contributed to manuscript revision, read, and approved the submitted version.

FUNDING

This work was supported by the National Natural Science Foundation of China (62075245).

SUPPLEMENTARY MATERIAL

The Supplementary Material for this article can be found online at: https://www.frontiersin.org/articles/10.3389/fenrg.2022.837160/full#supplementary-material

REFERENCES

Abdul Bashid, H. A., Lim, H. N., Kamaruzaman, S., Abdul Rashid, S., Yunus, R., Huang, N. M., et al. (2017). Electrodeposition of Polypyrrole and Reduced Graphene Oxide onto Carbon Bundle Fibre as Electrode for Supercapacitor. *Nanoscale Res. Lett.* 12, 246–24610. doi:10.1186/s11671-017-2010-3

Bai, X., Liu, Q., Liu, J., Gao, Z., Zhang, H., Chen, R., et al. (2017). All-solid State Asymmetric Supercapacitor Based on NiCoAl Layered Double Hydroxide Nanopetals on Robust 3D Graphene and Modified Mesoporous Carbon. *Chem. Eng. J.* 328, 873–883. doi:10.1016/j.cej.2017.07.118

Bashiri-Shahroodi, A., Nassab, P. R., Szabó-Révész, P., and Rajkó, R. (2008). Preparation of a Solid Dispersion by a Dropping Methodto Improve the Rate of Dissolution of Meloxicam. *Drug Dev. Ind. Pharm.* 34, 781–788. doi:10.1080/03639040801925735

Brousse, T., B´elanger, D., and Long, J. W. (2015). To Be or Not to Be Pseudocapacitive? *J. Electrochem. Soc.* 162, 5185–5189. doi:10.1149/2.0201505jes

Ding, S., Du, X., Yang, Y., Wang, P., Zhang, Z., Hao, X., et al. (2018). Theoretical and Experimental Investigation of Electronic/ionic Conductivity and Deprotonation of $Ni_{3-x}Co_xAl$-LDHs in an Electrochemical Energy Storage System. *Phys. Chem. Chem. Phys.* 20, 173131–173233. doi:10.1039/c8cp01247d

Dubal, D. P., Lee, S. H., Kim, J. G., Kim, W. B., and Lokhande, C. D. (2012). Porous Polypyrrole Clusters Prepared by Electropolymerization for a High Performance Supercapacitor. *J. Mater. Chem.* 22, 3044–3052. doi:10.1039/c2jm14470k

Gao, X., Liu, X., Wu, D., Qian, B., Kou, Z., Pan, Z., et al. (2019). Significant Role of Al in Ternary Layered Double Hydroxides for Enhancing Electrochemical Performance of Flexible Asymmetric Supercapacitor. *Adv. Funct. Mater.* 29, 190387901–190387912. doi:10.1002/adfm.201903879

Gonçalves, J. M., Silva, M. I., Toma, H. E., Angnes, L., Martins, P. R., Araki, K., et al. (2020). Trimetallic Oxides/hydroxides as Hybrid Supercapacitors Electrode Materials: A Review. *J. Mater. Chem. A* 8, 10534–10570. doi:10.1039/D0TA02939D

Gopalakrishnan, M., Srikesh, G., Mohan, A., and Arivazhagan, V. (2017). *In-situ* Synthesis of Co_3O_4/graphite Nanocomposite for High-Performance Supercapacitor Electrode Applications. *Appl. Surf. Sci.* 403, 578–583. doi:10.1016/j.apsusc.2017.01.092

Gu, C. D., Ge, X., Wang, X. L., and Tu, J. P. (2015). Cation-anion Double Hydrolysis Derived Layered Single Metal Hydroxide Superstructures for Boosted Supercapacitive Energy Storage. *J. Mater. Chem. A.* 3, 14228–14238. doi:10.1039/c5ta03140k

Guo, D., Song, X., Tan, L., Ma, H., Sun, W., Pang, H., et al. (2019). A Facile Dissolved and Reassembled Strategy towards sandwich-like rGO@NiCoAl-LDHs with Excellent Supercapacitor Performance. *Chem. Eng. J.* 356, 955–963. doi:10.1016/j.cej.2018.09.101

Gupta, V., Gupta, S., and Miura, N. (2009). Electrochemically Synthesized Large Area Network of CoxNiyAlz Layered Triple Hydroxides Nanosheets: A High Performance Supercapacitor. *J. Power Sourc.* 189, 1292–1295. doi:10.1016/j.jpowsour.2009.01.026

He, F., Hu, Z., Liu, K., Guo, H., Zhang, S., Liu, H., et al. (2015). Facile Fabrication of GNS/NiCoAl-LDH Composite as an Advanced Electrode Material for High-

Performance Supercapacitors. *J. Solid State. Electrochem.* 19, 607–617. doi:10.1007/s10008-014-2644-3

Hou, L., Du, Q., Su, L., Di, S., Ma, Z., Chen, L., et al. (2018). Ni-Co Layered Double Hydroxide with Self-Assembled Urchin like Morphology for Asymmetric Supercapacitors. *Mater. Lett.* 237, 262–265. doi:10.1016/j.matlet.2018.11.123

Huang, L., Liu, B., Hou, H., Wu, L., Zhu, X., Hu, J., et al. (2018). Facile Preparation of Flower-like NiMn Layered Double Hydroxide/reduced Graphene Oxide Microsphere Composite for High-Performance Asymmetric Supercapacitors. *J. Alloys Comp.* 730, 71–80. doi:10.1016/j.jallcom.2017.09.195

Kim, J. Y., Lee, S.-H., Yan, Y., Oh, J., and Zhu, K. (2012). Controlled Synthesis of Aligned Ni-NiO Core-Shell Nanowire Arrays on Glass Substrates as a New Supercapacitor Electrode. *RSC Adv.* 2, 8281–8285. doi:10.1039/c2ra20947k

Le, V. T., Kim, H., Ghosh, A., Kim, J., Chang, J., Vu, Q. A., et al. (2013). Coaxial Fiber Supercapacitor Using All-Carbon Material Electrodes. *ACS Nano* 7, 5940–5947. doi:10.1021/nn4016345

Li, T., Li, G. H., Li, L. H., Liu, L., Xu, Y., Ding, H. Y., et al. (2016). Large-scale Self-Assembly of 3D Flower-like Hierarchical Ni/Co-LDHs Microspheres for High-Performance Flexible Asymmetric Supercapacitors. *ACS Appl. Mater. Inter.* 8, 2562–2572. doi:10.1021/acsami.5b10158

Li, X., Wu, H., Guan, C., Elshahawy, A. M., Dong, Y., Pennycook, S. J., et al. (2018). (Ni,Co)Se_2/NiCo-LDH Core/shell Structural Electrode with the Cactus-like (Ni,Co)Se_2 Core for Asymmetric Supercapacitors. *Small* 15, 180389501–180389510. doi:10.1002/smll.201803895

Li, Y., Gan, K., Huo, W., Liu, K., Liu, J., Wang, X., et al. (2019). Novel Design of High-Surface-Area Poly-Hollow Alumina Spheres via a Facile ball Dropping Method Based on Particle-Stabilized Emulsions. *Ceramics Int.* 45, 22940–22947. doi:10.1016/j.ceramint.2019.07.337

Pan, D., Ge, S., Zhao, J., Shao, Q., Guo, L., Zhang, X., et al. (2018). Synthesis, Characterization and Photocatalytic Activity of Mixed-Metal Oxides Derived from NiCoFe Ternary Layered Double Hydroxides. *Dalton Trans.* 47, 9765–9778. doi:10.1039/c8dt01045e

Patil, S. J., Kim, J. H., and Lee, D. W. (2017). Self-assembled Ni 3 S 2//CoNi 2 S 4 Nanoarrays for Ultra High-Performance Supercapacitor. *Chem. Eng. J.* 322, 498–509. doi:10.1016/j.cej.2017.03.095

Raj, K., Soni, P., and Siril, P. F. (2019). Engineering the Morphology and Particle Size of High Energetic Compounds Using Drop-By-Drop and Drop-To-Drop Solvent-Antisolvent Interaction Methods. *ACS Omega* 4, 5424–5433. doi:10.1021/acsomega.8b03214

Shang, S., Hanif, A., Sun, M., Tian, Y., Ok, Y. S., Yu, I. K. M., et al. (2019). Novel M (Mg/Ni/Cu)-Al-CO3 Layered Double Hydroxides Synthesized by Aqueous Miscible Organic Solvent Treatment (AMOST) Method for CO2 Capture. *J. Hazard. Mater.* 373, 285–293. doi:10.1016/j.jhazmat.2019.03.077

Sharonova, A., Loza, K., Surmeneva, M., Surmenev, R., Prymak, O., and Epple, M. (2016). Synthesis of Positively and Negatively Charged Silver Nanoparticles and Their Deposition on the Surface of Titanium. *IOP Conf. Ser. Mater. Sci. Eng.* 116, 012009. doi:10.1088/1757-899x/116/1/012009

Sokol, D., Vieira, D. E. L., Zarkov, A., Ferreira, M. G. S., Beganskiene, A., Rubanik, V. V., et al. (2019). Sonication Accelerated Formation of Mg-Al-Phosphate Layered Double Hydroxide via Sol-Gel Prepared Mixed Metal Oxides. *Sci. Rep.* 9, 10419–1041909. doi:10.1038/s41598-019-46910-5

Su, L., Yu, X., Miao, Y., Mao, G., Dong, W., Feng, S., et al. (2019). Alkaline-promoted Regulation of the Peroxidase-like Activity of Ni/Co LDHs and Development Bioassays. *Talanta* 197, 181–188. doi:10.1016/j.talanta.2019.01.021

Tan, S., Li, J., Zhou, L., Chen, P., Shi, J., and Xu, Z. (2018). Modified Carbon Fiber Paper-Based Electrodes Wrapped by Conducting Polymers with Enhanced Electrochemical Performance for Supercapacitors. *Polymers (Basel)* 10, 107201–107210. doi:10.3390/polym10101072

Theiss, F. L., Ayoko, G. A., and Frost, R. L. (2016). Synthesis of Layered Double Hydroxides Containing Mg2+, Zn2+, Ca2+ and Al3+ Layer Cations by Co-precipitation Methods-A Review. *Appl. Surf. Sci.* 383, 200–213. doi:10.1016/j.apsusc.2016.04.150

Tian, Y., Zhu, L., Shang, M., Han, E., and Song, M. (2020). Effect of Soft Templating Agent on NiCoAl-LDHs Grown *In Situ* on Foamed Nickel for High-Performance Asymmetric Supercapacitors. *Ionics* 26, 1431–1442. doi:10.1007/s11581-019-03282-0

Tyagi, A., Joshi, M. C., Shah, A., Thakur, V. K., and Gupta, R. K. (2019). Hydrothermally Tailored Three-Dimensional Ni-V Layered Double Hydroxide Nanosheets as High-Performance Hybrid Supercapacitor Applications. *ACS omega* 4, 3257–3267. doi:10.1021/acsomega.8b03618

Wang, H., Liu, X., Wu, Y., Hou, C., Qiu, Y., and Guo, K. (2017b). Microwave-assisted Synthesis of Ethylene Glycol-Intercalated NiAl LDHs and Their Application for Intracrystalline Catalytic Esterification with Naphthenic Acids in Crude Oil. *Energy Fuels* 31, 9898–9904. doi:10.1021/acs.energyfuels.7b01424

Wang, M., Xue, J., Zhang, F., Ma, W., and Cui, H. (2015). Facile Synthesis of Nickel–Cobalt Double Hydroxide Nanosheets with High Rate Capability for Application in Supercapacitor. *J. Nanoparticle Res.* 17, 1061–1069. doi:10.1007/s11051-015-2918-4

Wang, X., Lin, Y., Su, Y., Zhang, B., Li, C., Wang, H., et al. (2017a). Design and Synthesis of Ternary-Component Layered Double Hydroxides for High-Performance Supercapacitors: Understanding the Role of Trivalent Metal Ions. *Electrochimica Acta* 225, 263–271. doi:10.1016/j.electacta.2016.12.160

Xiang, W., Zhang, J., Liu, Y., Hu, M., Zhao, K., Guo, H., et al. (2017). Facile Controlled Synthesis and Magnetic Properties of High-Aspect-Ratio Nickel Nanowires Prepared by the Dropping Method. *J. Alloys Comp.* 693, 257–263. doi:10.1016/j.jallcom.2016.09.145

Xu, J., Gai, S., He, F., Niu, N., Gao, P., Chen, Y., et al. (2014). Reduced Graphene oxide/Ni1−xCoxAl-Layered Double Hydroxide Composites: Preparation and High Supercapacitor Performance. *Dalton Trans.* 43, 11667–11675. doi:10.1039/c4dt00686k

Yang, L., Xu, J., Feng, T., Yao, Q., Xie, J., and Xia, H. (2017). Fe_2O_3 Nanoneedles on Ultrafine Nickel Nanotube Arrays as Efficient Anode for High-Performance Asymmetric Supercapacitors. *Adv. Funct. Mater.* 27, 160672801–160672810. doi:10.1002/adfm.201606728

Yang, S.-S., Xie, M.-J., Shen, Y., Wang, Y.-Z., Guo, X.-F., and Shen, B. (2016). Ni-Al Composite Hydroxides Fabricated by Cation-Anion Double Hydrolysis Method for High-Performance Supercapacitor. *Chin. Chem. Lett.* 27, 507–510. doi:10.1016/j.cclet.2016.01.058

Zhang, H., Usman Tahir, M., Yan, X., Liu, X., Su, X., and Zhang, L. (2019). Ni-Al Layered Double Hydroxide with Regulated Interlayer Spacing as Electrode for Aqueous Asymmetric Supercapacitor. *Chem. Eng. J.* 368, 905–913. doi:10.1016/j.cej.2019.03.041

Zhang, Y., Wang, J., Yu, L., Wang, L., Wan, P., Wei, H., et al. (2017). Ni@NiCo2O4 Core/shells Composite as Electrode Material for Supercapacitor. *Ceramics Int.* 43, 2057–2062. doi:10.1016/j.ceramint.2016.10.179

Zheng, C.-H., Yao, T., Xu, T.-R., Wang, H.-A., Huang, P.-F., Yan, Y., et al. (2016). Growth of Ultrathin Ni Co Al Layered Double Hydroxide on Reduced Graphene Oxide and Superb Supercapacitive Performance of the Resulting Composite. *J. Alloys Comp.* 678, 93–101. doi:10.1016/j.jallcom.2016.03.293

Conflict of Interest: The authors declare that the research was conducted in the absence of any commercial or financial relationships that could be construed as a potential conflict of interest.

Publisher's Note: All claims expressed in this article are solely those of the authors and do not necessarily represent those of their affiliated organizations or those of the publisher, the editors, and the reviewers. Any product that may be evaluated in this article or claim that may be made by its manufacturer is not guaranteed or endorsed by the publisher.